JACS
JOURNAL OF THE AMERICAN CHEMICAL SOCIETY
Article
pubs.acs.org/JACS

Pressure Modulation of the Enzymatic Activity of Phospholipase A2, A Putative Membrane-Associated Pressure Sensor

Saba Suladze, Suleyman Cinar, Benjamin Sperlich, and Roland Winter*

Department of Chemistry and Chemical Biology, Biophysical Chemistry, TU Dortmund University, Otto-Hahn-Str. 6, D-44221 Dortmund, Germany

Supporting Information

ABSTRACT: Phospholipases A2 (PLA2) catalyze the hydrolysis reaction of sn-2 fatty acids of membrane phospholipids and are also involved in receptor signaling and transcriptional pathways. Here, we used pressure modulation of the PLA2 activity and of the membrane's physical−chemical properties to reveal new mechanistic information about the membrane association and subsequent enzymatic reaction of PLA2. Although the effect of high hydrostatic pressure (HHP) on aqueous soluble and integral membrane proteins has been investigated to some extent, its effect on enzymatic reactions operating at the water/lipid interface has not been explored, yet. This study focuses on the effect of HHP on the structure, membrane binding and enzymatic activity of membrane-associated bee venom PLA2, covering a pressure range up to 2 kbar. To this end, high-pressure Fourier-transform infrared and high-pressure stopped-flow fluorescence spectroscopies were applied. The results show that PLA2 binding to model biomembranes is not significantly affected by pressure and occurs in at least two kinetically distinct steps. Followed by fast initial membrane association, structural reorganization of α-helical segments of PLA2 takes place at the lipid water interface. FRET-based activity measurements reveal that pressure has a marked inhibitory effect on the lipid hydrolysis rate, which decreases by 75% upon compression up to 2 kbar. Lipid hydrolysis under extreme environmental conditions, such as those encountered in the deep sea where pressures up to the kbar-level are encountered, is hence markedly affected by HHP, rendering PLA2, next to being a primary osmosensor, a good candidate for a sensitive pressure sensor in vivo.

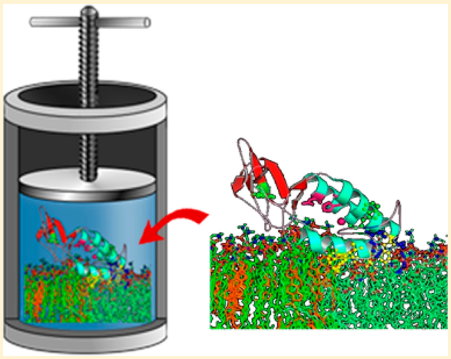

INTRODUCTION

Biomembranes play a key role in regulating a wide range of cellular processes by providing an active two-dimensional lipid matrix within which biochemical reactions can occur. The structure and dynamic lateral organization of these membranes selectively modulate the activity of membrane associated proteins, such as receptors and channels.[1−3] One important class of membrane associated proteins are phospholipases. On the basis of their cellular location, phospholipases are generally divided into two groups: 14−16 kDa secretory PLA2 (sPLA2) and 80−85 kDa intracellular PLA2s.[4] The structure of sPLA2 is dominated by three α-helices, two of them coupled by an antiparallel β-sheet. This assembly forms a hydrophobic channel that extends from the surface of the molecule to the active site, allowing incorporation of a lipid substrate molecule to access the catalytic site. The protein's main structural features also include the catalytic Asp-His dyad, the calcium binding loop, and the interfacial binding site with its hydrogen bonding network, which is responsible for the attachment of the protein to the lipid membrane.[5] For phospholipid hydrolysis, PLA2s require to bind to the membrane-water interface. The rates of interfacial activation and hydrolysis are influenced by the membrane's physical−chemical properties, including membrane curvature, compressibility, lateral diffusivity, surface charge, and hydration.[6,7] In contrast to varying interface binding surfaces of the enzymes across sPLA2 members,[8] the active site structure, residues involved in calcium binding and catalysis, as well as orientations of the catalytic water are highly conserved,[5] implying common modes of their reaction. While PLA2s are attractive targets for pharmacological applications,[9] the relationship between their mechanistic action and physiological function remains still poorly characterized.[10]

Using pressure modulation of the activity of PLA2 and of the membrane's physical−chemical properties, one aim of this work was to reveal novel kinetic and mechanistic information about the membrane association process and subsequent reaction of the enzyme. In fact, the interest in using, next to temperature and chemical potential (or activity), pressure as a thermodynamic and kinetic variable has been largely growing in physical−chemical studies of biological systems in recent years.[11,12] Generally, pressure acts on the structure and dynamics of biomolecular systems through changes in specific volume that are largely due to changes in hydration or packing efficiency. Thus, high hydrostatic pressure (HHP) is uniquely well suited for studying the role of solvation in folding, dynamics and interactions of proteins and other biomolecules. Moreover, high pressure may increase the population of so far

Received: July 6, 2015
Published: September 14, 2015

DOI: 10.1021/jacs.5b07009
J. Am. Chem. Soc. 2015, 137, 12588−12596

undetected excited states (e.g., conformational and functional substates) and allows modulating biochemical processes, thereby enabling determination of reaction constants which otherwise cannot be obtained.[13]

Besides the general physical−chemical interest in using high pressure as a tool for understanding the structure, phase behavior and energetics of biomolecules, HHP is also of biotechnological (e.g., for steering enzymatic processes by pressure modulation, for which the term baroenzymology has been coined) and physiological (e.g., for understanding the physiology of deep-sea organisms living in cold and high-pressure habitats) interest. Interestingly, though the biological membrane seems to be one the most pressure sensitive biological system,[12−17] pressure effects on binding and activity changes of membrane associated proteins are largely unknown. In particular mechanisms how external pressure stress is sensed and how this information is transferred in organisms being exposed to high pressure stress are still largely unknown. Membrane stretch-activated sensors, membrane-localized proteins whose activities are modulated by mechanical forces generated in the membrane, appear to be promising candidates for the role of detecting changes in external stress.[18−22] Various kinds of environmental stresses, such as temperature stress, osmotic and hydrostatic pressure stress, cause severe alterations in the physical properties of the membrane lipids in model membranes and in living cell membranes. In particular, dynamic properties and the membrane's lateral organization are significantly altered upon compression.[23] Hence, promising candidates for the role of detecting changes in external stress, such as pressure, include mechanosensitive ion channels and membrane-localized enzymes such as phospholipase A2 (PLA2). The activity of PLA2 is sensitive to packing of the lipid bilayer of the cell and is responsive to osmotic changes, i.e., will be a prime candidate to look into pressure effects as well. As the rates of interfacial activation and hydrolysis will be significantly influenced by the membrane's physical−chemical properties, marked pressure effects can be envisioned.[1−3] As the lipid head groups region is relatively incompressible compared to the hydrocarbon interior, pressure affects membrane function essentially by increasing the packing density and order parameter of lipid chains and, for heterogeneous membranes, their lateral organization.[24,25] Furthermore, pressure can affect membrane-associated processes by modulation of the membrane protein's conformational substates and altering interactions of these proteins with membrane components, ligands and receptors.[13,20]

Phospholipases A2 superfamily enzymes are involved in regulatory processes as they interact directly with the membrane by altering both its chemical composition and physical state by hydrolysis of the sn-2 ester bond of phospholipids to produce free fatty acids (arachidonic acid) and lysophospholipids, which take part in cell signaling, immune system responses against bacterial infections and stimulation of inflammations.[26−31] As they play an important role in membrane remodeling processes as well as in cellular signaling cascades, they should be able to serve as effective pressure sensor. Hence, as a second aim of this study, we set out to explore the pressure sensitivity of bee venom phospholipase A2, bvPLA2, and study its binding process and enzymatic activity upon HHP stress using appropriate model biomembrane systems. To this end, we used a rapid mixing high-pressure stopped-flow spectroscopy platform, which enabled us to obtained new structural, thermodynamic and kinetic information on the action of PLA2 in various model biomembrane systems at HHP conditions. We demonstrate that the rate of the PLA2-membrane penetration is not significantly influenced by pressure. In contrast, the application of pressure drastically inhibits the activity of the membrane-attached enzyme, rendering it a potentially effective pressure sensing system. Moreover, our results deepen our understanding of membrane-associated pressure effects in deep-sea organisms, where pressures up to the kbar-level are encountered.

RESULTS

Effect of Pressure on the Conformation of BvPLA2 in Bulk Solution and upon Membrane Binding. To reveal the pressure stability of the enzyme first, we measured high-pressure FTIR spectra of bvPLA2 in the pressure range from 1 bar to 10 kbar and analyzed the pressure-induced changes in the amide I′ spectral region of the protein (Figures 1a,b, S1). The second derivative spectra of the amide I′ band allow a better visualization of the changes occurring and are shown here in Figure 1c,d for the protein in bulk solution and in the presence of a lipid bilayer. BvPLA2 displays an amide I′ band contour with similar contents of stable α-helices and β-sheets as well as β-turns and random coil secondary structures, in good

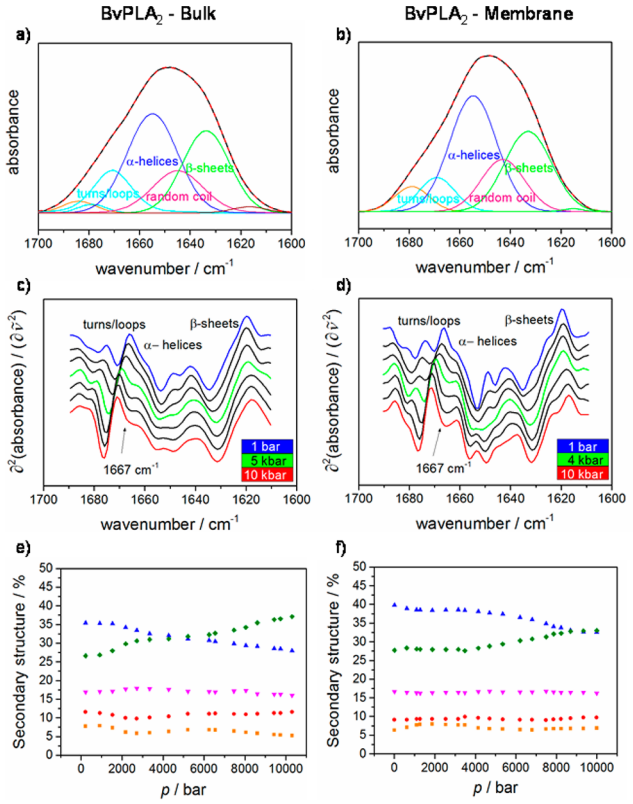

Figure 1. Pressure-induced changes in the amide I′ spectra, their second derivative and curve fitting results of the FTIR data at 1 bar for bvPLA2 in bulk solution (a,c,e) and in the presence of the lipid bilayer (b,d,f). The raw FTIR spectrum is shown in black, the fitted spectrum in red, and the component bands assigned to the secondary structure elements are marked as well according to the assignment given in Table S1. Secondary structural changes (▲ α-helices, ◆ β-sheets, ▼ random structures, ● and ■ turns and loops) of bvPLA2 as a function of pressure at 37 °C in (e) bulk solution and (f) in the presence of the lipid bilayer.

DOI: 10.1021/jacs.5b07009
J. Am. Chem. Soc. 2015, 137, 12588−12596

agreement with the X-ray crystal structure data (Table S1). The bvPLA2 protein maintains its compact tertiary structure even at high pressures of 10 kbar, indicating a high pressure stability of this protein. Linear pressure-induced frequency shifts (elastic effects) are frequently observed as a result of pressure-induced compression of the chemical bonds equivalent to changes of the force constant. All secondary structural elements except β-sheets exhibit this blue shift. The band position for intramolecular β-sheets observed at 1635 cm^{-1} remains constant throughout the entire pressure range, indicating the absence of solvent exposed β-sheets up to 10 kbar.[13] Only small, but reversible changes in spectral shape are visible upon pressurization (Figures 1c,d, S1), which renders bvPLA2 a very attractive model for detailed high-pressure enzymological studies of membrane associated proteins. For bvPLA2 in bulk solution, we notice a small decrease is the observed α-helical content upon compression with a concomitant increase of β-sheets, but the contribution of unordered secondary structure elements does not increase. At pressures above ~5 kbar, a subband appears at 1667 cm^{-1}, suggesting pressure-induced formation of solvated turns/loops.[32] The pressure-induced secondary structural changes can be more easily monitored by means of a quantitative fit analysis of the amide I′ band region using mixed Gaussian and Lorentzian line shapes for deconvolution. As can be deduced from Figure 1e,f, the α-helix content deceases by about 7%, and intramolecular β-sheets increase concomitantly by about 10% altogether. Hence, these data indicate a minor pressure-induced shift toward more β-sheets at the expense of α-helices in the high-pressure state of the protein.

Members of the sPLA2s are activated by attaching to the plasma membrane, thereby rendering the membrane interaction of the bvPLA2 proteins crucial for their function. Therefore, the effect of membrane binding on the pressure-induced conformational changes needs to be explored and compared with the bulk solution behavior. FTIR amide I′ spectra were recorded for bvPLA2 bound to the anionic model raft membrane DOPC/DOPG/DPPC/DPPG/Chol 20:5:45:5:25 (molar ratio) under noncatalytic conditions. We observe small secondary structural changes in the protein upon membrane binding at ambient pressure (Figure 1a,b). Changes are mainly observed in the α-helical regions when compared to the bulk behavior, suggesting their involvement in membrane binding. This result is consistent with earlier observations by Pande et al., showing that bvPLA2 predominately exhibits membrane interaction through the helical region that is lying at the lipid interface (Figure 2).[33] The α-helical peak at 1651 cm^{-1} has also been found to split into two subcomponents at ~1650 and ~1658 cm^{-1} in the presence of POPC/POPG lipid vesicles, the latter supposed to being due to a flexible, more dynamic α-helix.[34] A subband for solvated turns/loops at 1667 cm^{-1} (minimum in the second derivative spectra) in the presence of membrane appears at rather low pressures, which becomes more clearly visible at higher pressures. This small difference compared to the bulk solution structure can be linked to formation of a more flexible conformation of the PLA2 upon membrane binding due to disruption of a few intrahelical hydrogen bonds and formation of such bonds between the enzyme and the phosphate, carbonyl, and hydroxyl groups of membrane lipids, resulting in stabilization of the transition-state complex for efficient catalysis.[34,35]

Figure 1d displays the variation of the secondary structural contents of membrane-bound bvPLA2 with increasing pressure.

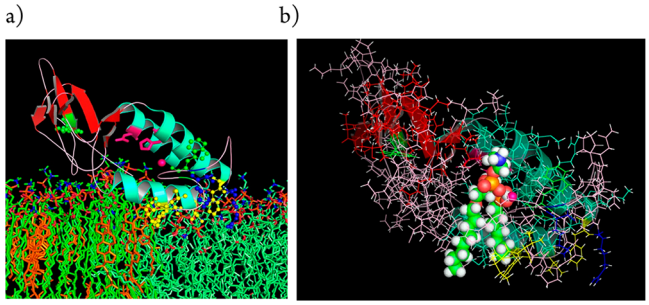

Figure 2. (a) Model of a lipid vesicle binding bvPLA2. The hydrophobic residues surrounding the substrate binding cleft and involved in membrane anchoring, Ile-1, Ile-2, Phe-24, Ile-78, and Phe-82, are colored in yellow, and the cationic residues that support membrane binding by ionic and/or H-bonding interactions with the lipid polar groups, Lyz-14, and Arg-23, are colored in blue. Trp-8 and Trp-128 are colored green (ball and stick format). The active site residues, the His-34 Asp-64 diad, and the bound Ca^{2+} are shown in magenta. BvPLA2 orientation to the membrane-water interface and the depth of insertion is accessed from.[33] (b) Bee venom phospholipase A2, bvPLA2, with a phosphonate transition-state analogue (1-*O*-octyl-2-heptylphosphonyl-*sn*-glycero-3-phosphoethanolamine) in the active site (pdb entry 1POC).[5] Atoms of the transition-state analogue are represented by colored spheres: C (green), H (white), O (red), P (gold), and N (blue).

For membrane-bound bvPLA2, upon compression, the helix content decreases by about 7%, similar to the bulk behavior, with a concomitant increase in β-sheets by 6%, whereas observed changes for unordered structures and turns/loops are less than 1%, i.e., insignificant within the accuracy of the experiment. Interestingly, these pressure-induced small conformational changes appear for the membrane associated protein at much higher pressures (>4 kbar) compared to the bulk (>~1.5 kbar), indicating strong stabilization of the conformation of bvPLA2 in its membrane-bound form (Figure 1e,f).

Membrane Association of BvPLA2. In order to study the association of PLA2 with liposomes, we used a fluorescence-based assay for the kinetic analysis of this interaction.[36] The spatial approximation of bvPLA2 to liposomes was detected by Förster resonance energy transfer (FRET) from the intrinsic protein tryptophans to a PC-based fluorescent dye (β-DPH HPC) embedded in the lipid bilayer, allowing emission to be observed in the range of 420−520 nm. The 15-kDa bvPLA2 protein has 2 tryptophan residues, at positions 8 and 128. Detected changes in the intensity of the fluorescent signal upon PLA2-liposome binding were in the range of 10−40% (Figure 3a,b).

The time course of the association process could be described by a biexponential function, implying that the bvPLA2-membrane interaction occurs in at least two steps. From a biexponential fit of the association curves at different lipid concentrations, the corresponding observed rate constants, $k_{obs,1}$ and $k_{obs,2}$, were derived and the binding kinetics quantified. For the interaction of 0.35 μM bvPLA2 with 62.5 μM lipids in unilamellar vesicles at 37 °C, the fast association process for the phase-separated anionic raft-like membrane, exhibiting liquid-ordered (l_o)/liquid-disordered(l_d) domain coexistence, revealed a rate, $k_{obs,1}$, of about 39 s^{-1}, which is almost 10 times higher than that of the slower process with a rate, $k_{obs,2}$, of about 3.0 s^{-1}. The second process contributed approximately 40% to the entire FRET signal increase (Figure

DOI: 10.1021/jacs.5b07009
J. Am. Chem. Soc. 2015, 137, 12588−12596

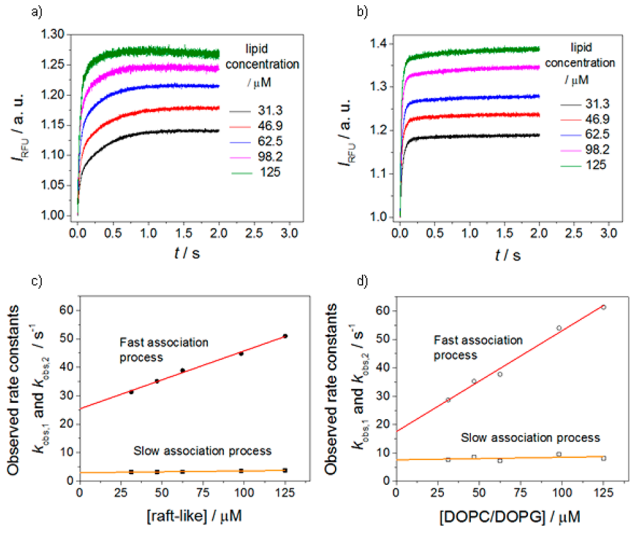

Figure 3. PLA2 binding to lipid membranes. Association curves expressed in relative fluorescence units (I_{RFU}) of a stopped-flow kinetic experiment with 0.35 μM bvPLA2 and increasing concentrations of liposomes, (a) anionic raft-like vesicles DOPC/DOPG/DPPC/DPPG/Chol/DPH-HPC 19/5/43/5/24/4 mol % and (b) DOPC/DOPG/DPH-HPC 86/10/4 mol %. The FRET measurements reveal a fast concentration-dependent and a slower concentration-independent association process for (c) the anionic raft-like and (d) the DOPC/DOPG lipid vesicles.

S2). Increasing the lipid concentration stepwise from 31.3 to 125 μM, with the concentration of PLA2 kept constant at 0.35 μM, displayed a marked increase of the fast association rate as a function of lipid concentration, ranging from 30 to 50 s^{-1}. The slower component, however, remained approximately constant at 3.0 s^{-1}, i.e., is essentially independent of the lipid concentration.

In a second experimental series, we studied bvPLA2 binding to the homogeneous anionic membrane DOPC/DOPG (lipid bilayer with a molar ratio 90/10) which exhibits an all-fluid (l_d) phase, only. We found that, in contrast to that of raft-like phase separated membranes, binding of PLA2 to vesicles composed of the DOPC/DOPG mixture displays an about 2-fold faster rate constant for $k_{obs,2}$ (about 7.5 s^{-1}), and this slower second process contributes only 10% to the entire FRET signal increase (Figure S2). The fast component $k_{obs,1}$ is of similar magnitude at low to medium lipid concentrations. A careful analysis of the slow binding kinetics of bvPLA2 to the heterogeneous anionic raft-like membrane with respect to the homogeneous DOPC/DOPG membrane reveals a more complex behavior, which might be due to effects of changes in localization and/or lipid sorting to reach a favorable fluid environment which is required for PLA2 function.

A linear fit to the observed rate constants ($k_{obs} = k_{on}$ [Lipid] + k_{off}) allowed the calculation of the dissociation constant, $K_{d,1} = k_{off,1}/k_{on,1}$, for the fast binding step 1. Taking into account that one bvPLA2 molecule is surrounded by about 20 lipids forming its binding site,[37] an apparent second-order association rate constant for the first rapid phase, k_{on}, was obtained from the slope of the plot shown in Figure 3c,d, yielding a value of $k_{on} = (0.203 \times 10^6\ M^{-1}\ s^{-1} \times 20) = 4.07 \times 10^6\ M^{-1}\ s^{-1}$ for the raft mixture, and the dissociation rate constant, k_{off}, from the intercept with the ordinate, amounts to 25.4 s^{-1}, which corresponds to a first-order rate constant for the reverse reaction. Hence, the fast membrane binding phase of bvPLA2 to raft-like lipid vesicles is associated with a $K_{d,1}$ value of 6.2 μM. Following the same considerations, a $K_{d,1}$ value of 2.5 μM was obtained for DOPC/DOPC vesicles. The overall process including the fast and slow phases of binding bvPLA2 to these model membranes is expected to proceed with a dissociation constant in the submicromolar range (K_d < 1 μM).[38]

Figure 4 displays the binding reaction of bvPLA2 to model membranes under HHP conditions, measured using the high-

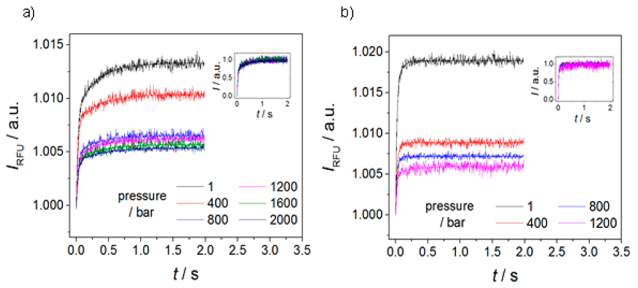

Figure 4. Pressure-independent PLA2 association kinetics to lipid bilayers composed of (a) the anionic raft-like and (b) DOPC/DOPG lipid vesicles. Thin solid lines represent double-exponential fits to the experimental data. The inset shows the intensity-normalized fluorescence curves.

pressure stopped-flow technique with fluorescence detection. Interestingly, pressure has a minor effect on the binding rate constant of PLA2 to the lipid membranes. The observed fast association rate observed in this high-pressures setup is in excellent agreement with the ambient-pressure stopped-flow data (Figure S2), yielding, for example, a value of $k_{obs,1}$ = 38 s^{-1} for the 62.5 μM lipid concentration at ambient pressure, which decreases slightly with increasing pressure, only. The inset of Figure 4 exhibits the overlap of normalized fluorescence curves for the different pressures studied, demonstrating the pressure-insensitivity of $k_{obs,1}$. The amplitude of the FRET signal of the binding process decreases markedly with pressure, however, implying a decrease in the equilibrium association constant, which may be due to a continuous increase in lipid chain packing upon pressurization. In fact, ^{2}H NMR-experiments on fluid lipid bilayers revealed a decrease of the chain-cross sectional area of about 10 Å^2/kbar.[39] However, the intrinsic pressure dependence of the fluorescence intensity of the β-DPH-HPC molecule suggests that a part of the observed effect may be due to the reduction of the emission intensity of the β-DPH-HPC fluorophore with increasing pressure (Figure S3).

Pressure Dependence of the Hydrolysis Reaction of BvPLA2. The kinetics of the hydrolysis reaction of phospholipid vesicles by PLA2s can be described by the Michaelis–Menten formalism.[8,40] Figure 5a,b display the reaction progress curves, i.e., the increase of Bodipy fluorescence of the reaction product with time, for the action of the bvPLA2 on lipid vesicles containing the heterogeneous raft-mixture and the homogeneous fluid-like DOPC/DOPG mixture, respectively. The rate of hydrolysis is enhanced as the substrate concentration increases and exhibits a curved dependence on lipid vesicle concentration. The initial rates of the corresponding data were fitted to the Lineweaver–Burk equation to determine the steady-state kinetic parameters K_M and k_{cat} of the enzyme (Figure 5c). While the Michaelis constant K_M is inversely proportional to the affinity or strength of a substrate binding to the active site of the enzyme, the turnover number, k_{cat}, provides information on the maximum

DOI: 10.1021/jacs.5b07009
J. Am. Chem. Soc. 2015, 137, 12588–12596

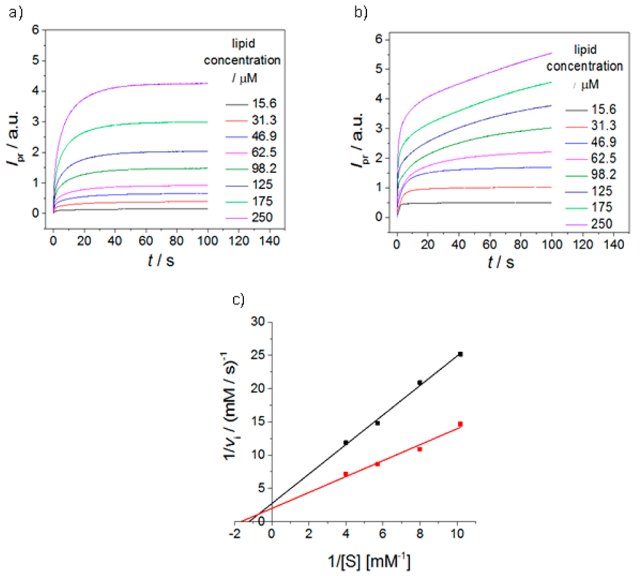

Figure 5. PLA2 activity in the presence of lipid membranes monitored by the fluorescence increase of the product (DBPC), I_{pr}, as determined by stopped-flow kinetic experiments using 0.35 μM bvPLA$_2$ and increasing concentrations of liposomes: (a) anionic raft membrane DOPC/DOPG/DPPC/DPPG/Chol/DBPC 19.5/5/44/5/24.5/1 mol %, and (b) homogeneous anionic bilayer DOPC/DOPG/DBPC 89/10/1 mol %. (c) Double reciprocal plot of the initial rate of hydrolysis as a function of substrate concentration, [S], for the anionic raft mixture (black) and the DOPC/DOPG membrane (red). Calibration was performed on the same samples after 24 h of the reaction, assuming full hydrolysis of the substrate.

number of molecules of substrate that an enzyme can convert to product. Precise quantification of the hydrolysis rate is difficult to assess as the available lipid substrate concentration is not easy to determine accurately. The PLA2 kinetics has been extensively studied based on the hydrolysis of only the phospholipids on the outer monolayer of the bilayer under the assumption that the enzyme is operating in a scooting mode (remains in the interface during thousands of catalytic cycles).[40,41] In contrast to these findings, a later study demonstrated that the reaction kinetics of bvPLA2 is also controlled by flip-flop process and both leaflets of the membrane are apparently hydrolyzed simultaneously.[42] Arbitrary units of the Bodipy containing product fluorescence signal were converted to μM s^{-1} by using calibration measurements on the same samples assuming full hydrolysis of the corresponding vesicles after 24 h of the reaction. The Lineweaver–Burk double-reciprocal plot of the kinetic data yield the following values for the anionic raft-like membrane: K_M = 0.8 mM, k_{cat} = 1048 s^{-1} and k_{cat}/K_M = 1.3 × 10^6 M s^{-1}, while for DOPC/DOPG vesicles values of K_M = 0.6 mM, k_{cat} = 1442 s^{-1}, and k_{cat}/K_M = 2.4 × 10^6 M s^{-1} are obtained, respectively. The k_{cat} values are 10–15 times larger in comparison to those of bvPLA2 on vesicles composed of 1,2-dimyristoylglycero-*sn*-3-phosphomethanol (DMPM) with blocked flip-flop.[41] The catalytic efficiency of the enzyme, k_{cat}/K_M, is comparable to that of human secretory PLA2.[43] PLA2 activation and the recognition of membrane lipids are believed to be largely determined by lipid protrusion.[44] The enzyme operating on the DOPC/DOPG model membrane substrate displayed a higher catalytic efficiency compared to that of the phase separated anionic raft-like mixture. This effect is probably due to a lower concentration of hydrolysis-competent disordered fluid lipid phase lipids in the heterogeneous membrane, which contains also 25% cholesterol, which is known to partially block the activation of PLA2.[45]

The effect of pressure on the activity of bvPLA2 was determined by measuring the steady-state enzyme kinetics at high pressure using rapid-mixing high-pressure stopped-flow (HPSF) methodology, which allows measurements up to 2 kbar with 2 ms time resolution and rapid fluorescence detection. Representative reaction traces for the two membrane systems are displayed in Figure 6a,b. The slope of the time-

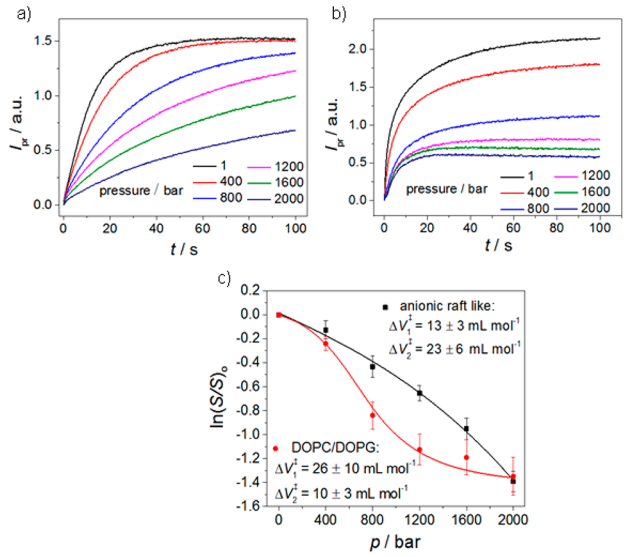

Figure 6. Effect of hydrostatic pressure on the rate of DBPC hydrolysis by bvPLA$_2$ for (a) anionic raft-like and (b) DOPC/DOPG lipid vesicles. (c) Pressure dependence of the enzymatic activity in the presence of anionic raft-like (black rectangles) and DOPC/DOPG (red circles) membrane. S and S_0 are the slopes of the fluorescence intensity as a function of time at pressure p and ambient pressure (1 bar), respectively.

dependent fluorescence change of the Bodipy-labeled reporter group in the reaction product decreases drastically with increasing pressure, indicating reduced hydrolysis rates upon pressurization. With respect to ambient pressure, the rate of the hydrolysis reaction decreases by a factor of 1.14 (~12% at 400 bar) at low and of 2.6 (~60% at 1600 bar) at high pressures in the model raft mixture, and by corresponding factors of 1.3 (~22%) and 3.3 (~70%), in the DOPC/DOPG membrane, respectively. As demonstrated by the FTIR data discussed at the beginning, these effects are not due to a pressure-induced denaturation of bvPLA2, which does not change its structure up to 4 kbar (Figure 1f). Analysis of Michaelis–Menten parameters for the pressure dependent study on the anionic raft-like membrane yields K_M values, which are within the experimental error bar of about 20% essentially independent of pressure, whereas k_{cat} decreases by a factor of 4–5 in the pressure range from 1 bar to 2 kbar.

The activation volume, i.e., the volume difference between the transition state and the reactants, $\Delta V^{\ddagger}$, can be deduced from the slope ($-\Delta V^{\ddagger}/RT$) of the ln(S/S_o) vs p plot (Figure 6c), where S is the slope of the fluorescence signal, $(dI_{pr}/dt)_p$, at pressure p relative to that at 1 bar, S_0.[46] As can be clearly seen, the effect of pressure on the rate of the reaction is nonlinear, rendering $\Delta V^{\ddagger}$ pressure dependent. $\Delta V^{\ddagger}$ for the enzyme activity in the anionic raft mixture increases from about 13 ± 3 mL

DOI: 10.1021/jacs.5b07009
J. Am. Chem. Soc. 2015, 137, 12588–12596

mol^{-1} at low pressures to 23 ± 6 mL mol^{-1} approaching 2 kbar. Corresponding values for the DOPC/DOPG lipid mixture amount to 26 ± 10 mL mol^{-1} and 10 ± 3 mL mol^{-1}, respectively. The positive $\Delta V^{\ddagger}$ values obtained reveal that the volume increases upon formation of the transition state. Alternatively, the pressure dependence of $\ln(S/S_o)$ can be analyzed using $\ln(k_{cat}/k_0) = -\Delta V^{\ddagger}p/(RT) + \Delta\kappa^{\ddagger}p^2/(2RT)$, i.e., by adding a compressibility term, where $\Delta\kappa^{\ddagger}$ is the activation compressibility, i.e., the partial molar compressibility difference between the transition and the reactant state. In this case, we yield a pressure independent activation volume for the anionic raft-like membrane of $\Delta V^{\ddagger}$ = 9 mL mol^{-1} and a negative $\Delta\kappa^{\ddagger}$ value of -8.7×10^{-3} mL mol^{-1} bar^{-1}, which reflects a larger compressibility of the enzyme–substrate complex compared to the transition state.

DISCUSSION AND CONCLUSIONS

In an attempt to better understand the structural-functional relationship of multifunctional PLA2s, including conditions of harsh environmental conditions such as high pressure, we explored the structure, binding and activity of the membrane-associated protein at atmospheric and high-pressure conditions by means of various biophysical methods. As demonstrated by our FTIR spectroscopic data, bvPLA2 is a very pressure-stable protein, displaying minor reversible conformational changes between about 1 bar and 10 kbar, only. A small decrease of α-helices is observed with a concomitant small increase of β-structures upon compression, only. Upon membrane binding, small conformational changes are observed by exposure of α-helical regions to the lipid interface. These data are in agreement with findings of Tatulian et al., who showed that the free enzyme in solution displays more resistance to amide $^1H/^2H$ exchange than the membrane-bound enzyme, suggesting an increase in flexibility in α-helical regions induced by snake venom PLA2 binding to lipid bilayers.[34] It has been proposed that more flexible helices are formed at the expense of disruption of a few intrahelical hydrogen bonds for membrane attachment and enzyme–substrate hydrogen bonding, leading to transition-state complex stabilization for efficient catalysis.[34,35] Membrane binding leads to an enhanced conformational stability of the protein, rendering the protein insensitive to conformational changes upon compression up to 4 kbar (Figure 1), which makes the system very suitable for studying pressure effects on its enzymatic activity.

Secretory PLAs are water-soluble enzymes that must adsorb to the substrate membrane interface for phospholipid hydrolysis to occur.[4] Even though the secreted enzymes exhibit similar catalytic mechanisms, for example with respect to the orientation of the catalytic water and the active site histidine and aspartate residues which are very similar in bvPLA2 and porcine pancreatic PLA2,[5] the mechanism of interfacial activation and specificity to membrane components upon binding seems to vary significantly. PLA2s with an excess of basic residues on the lipid binding surface display the strongest affinity toward negatively charged lipid surfaces, and PLA2s containing a tryptophan in the lipid binding surface display strong affinity toward neutral lipid substrates.[47] It has been suggested that binding of bvPLA2 to phospholipids occurs predominately in a nonelectrostatic fashion with hydrophobic interactions together with hydrogen-bonding providing a major portion of the interfacial binding energy.[37,38] Hydrophobic and basic residues of bvPLA2 involved in membrane anchoring are depicted in Figure 2. Additionally, interfacial activation is affected by membrane fluidity and curvature,[41,48] which are known to be largely affected by temperature and pressure.[23,49] Interestingly, the activity of bvPLA2 appears to be less sensitive to membrane fluidity. Substitution of DOPC with the more rigid POPC decreases the activity by only 8% in contrast to a 51% reduction of porcine pancreatic PLA2.[50] The reason might be that bvPLA2 does not penetrate as deep into the hydrocarbon core of the lipid bilayer like other PLA2s such as porcine pancreatic or human PLA2s do.[33,51] It has been suggested that isoform-specific differences in membrane-binding modes between PLA2s are likely related to their mechanistic differences.[33]

The stopped-flow kinetic binding studies illustrate that membrane-association of bvPLA2 can be explained using a two-step model in which a substrate concentration dependent fast phase is followed by a slower concentration independent process. For the interaction of 0.35 μM bvPLA2 with 62.5 μM lipids in raft-like liposomes, the fast association process displayed a rate (k_1) approximately 10-fold higher than that of slower process, with a rate (k_2) of about 3.0 s^{-1}. The fast step should involve the initial attachment of the enzyme upon binding to the lipid vesicles, while the slower second phase is expected to represent the reorientation of the enzyme at the lipid interface in a catalytically productive manner, involving structural rearrangements of α-helical regions of the bvPLA2 as observed in the FTIR measurements. In the case of the heterogeneous raft-like lipid mixture, it is very likely that the slower process involves also lipid sorting and lateral diffusion to ensure a suitable lipid environment for optimal function of the bvPLA2. In heterogeneous phase-separated model membranes, phase boundaries are believed to be a preferential site of phospholipase action.[7,48,52]

Using fluorescence resonance energy transfer from the PLA2 tryptophan residue to DPH-labeled membranes revealed that pressure does not significantly affect the rate of PLA2 binding to the membranes. Considering that charges and the hydration of the membrane surface and also the packing of the lipid head groups are not expected to change markedly in the 1–2000 bar pressure range,[24] a high packing efficiency of the protein with the membrane interface seems to be mainly responsible for the pressure independence of the association rate and the high stability of the membrane-bound protein, which forms a tight complex. Other studies revealed that membrane-associated mellitin and phospholipase Cβ are unaffected by pressure, concluding that previously observed displacement of integral membrane proteins with hydrostatic pressure are not a primary effect of increased lipid packing.[53,54]

The interfacial binding surface of the sPLA2 is distinct from the active site (Figure 2). Typically, the membrane attached enzyme can be found in three states: without bound substrate in its active site, with a substrate phospholipid molecule forming a classical Michaelis complex, or with bound product.[41] Generally, PLA2 specificity to substrate is regulated by a combination of two factors. First, PLA2's ability of membrane surface binding (E ↔ E*), which is related to an equilibrium dissociation constant. Second, after attachment to the membrane surface, the rate of hydrolysis of different substrates species by E* is governed by the relative interfacial specificity constant (k^*_{cat}/K^*_M), where K^*_M is related to the strength of PLA2 binding to a substrate molecule in its active site upon E*S complex formation (E*+S ↔ E*S), while k^*_{cat} displays the rate constant for the breakdown of the E*S complex (E*S → E

DOI: 10.1021/jacs.5b07009
J. Am. Chem. Soc. 2015, 137, 12588–12596

+P).[4] Hence, binding and activity should be studied separately for allowing a detailed interpretation of PLA2 action.

We determined the effect of pressure on the activity of bvPLA2 using an efficient fluorescence dequenching assay with the DBPC fluorophore incorporated into the anionic raft-like and DOPC/DOPG bilayers. To directly proof the heterogeneity of the raft-membrane and to visualize the action upon addition of PLA2, we carried out atomic force microscopy (AFM) measurements (Figure S4). In fact, the hydrolysis reaction has a dramatic effect on the lateral organization of the raft domain, finally leading to a complete loss of the lipid phase separation and to formation of holes in the lipid bilayer due to desorption of product molecules (see SI).

The overall characteristics of the membrane, including lipid packing, curvature, cholesterol level as well as phase separation into domains of different lipid order and fluidity have been shown to have a marked influence on PLA2 activation and hydrolysis.[7,48,55] As pressure has a marked effect on all these parameters,[33,51] pressurization is expected to largely control the hydrolysis rate of PLA2s. In particular, lipid bilayer thickness, dynamic properties and the membrane's lateral organization are significantly altered upon compression.[23,56] For example, membranes may contain lipid domains, i.e., aggregates of lipids in liquid-ordered (l_o) phases dispersed in liquid-disordered (l_d) phase lipids. The l_o phase is characterized by tight chain packing, reduced fluidity, high cholesterol level and extended lipid chains, although the lipid mobility is still high. Since high pressure promotes chain order, the application of pressure diminishes the disordered domains and the physical properties of the phases will become increasingly similar to pressure. Such scenario is expected to occur in our model raft mixture,[56] but domain coexistence is still persisting up to the 2 kbar region as applied here.[25] Conversely, DOPC vesicles remain in the liquid-disordered state under all studied pressure conditions, owing to its very low gel-to-fluid transition temperature ($T_m \approx -20$ °C).[57] The lipid bilayer thickness increases by about 1 Å kbar^{-1} in the liquid-like phase, only.[39]

Under atmospheric pressure conditions, the enzyme operating on DOPC/DOPG model membrane substrate displayed a higher catalytic efficiency compared to that of the phase separated anionic raft-like mixture (Figure 5c). Since the structure of bvPLA2 remains unperturbed up to 2 kbar, changes in activity upon pressure application should mainly result from the activation of the bvPLA2-phospholipid complex. If the transition state has a molecular volume different from that of the total volume of the reactants, i.e., $V(E+S) \neq V(ES^{\ddagger})$, a volume change in forming the activated complex can be directly measured from the pressure dependence of the rate constant k_{cat} (Figure 6). Clearly, a positive activation volume, $\Delta V^{\ddagger}$, of 13−26 mL mol^{-1} indicates that pressure creates an elastic barrier to transformation by favoring the smaller-volume reactant state. Further interpretation of the sign and magnitude of the activation volume is not a straightforward task because the experimentally obtained value can be represented by the sum of various contributions, including (i) intrinsic structural changes that result from disruption or formation of new bonds, (ii) solvation changes, which is often the dominating contribution that arises from the rearrangement of water molecules around interacting groups in the course of the reaction,[58] which is especially prominent when charge and dipole changes occur in the reacting molecules, and (iii) a substrate-induced volume change of the enzyme's conformation associated with chemical steps of the reaction, which includes possible changes in size of cavities and voids.[11,58] The proposed mechanism of PLA2 catalysis by Scott et al. suggests that the transition state is stabilized by displacement of two water molecules to the bulk solvent, while no significant deformation of the enzyme structure is required to achieve substrate transfer to the productive binding mode.[59] Clearly, release of two tightly bound water molecules from the active site of enzyme to the bulk can increase the net volume of the transition state. On the other hand, it has been shown that the interfacial activation of the enzyme involves allosteric coupling between the membrane-binding site and the catalytic center of PLA2.[6,60] The latter mechanism could involve creation of cavities, i.e., void volume, to the observed overall volume increase upon formation of the transition state.

To conclude, in this work we have investigated the structure, membrane binding and catalytic activity of bvPLA2 using pressure modulation and changes in membrane's physical−chemical properties. We could show that the PLA2 binding kinetics to model membranes is not markedly affected by pressure even up to 2 kbar and occurs in at least two kinetically distinct steps. Followed by fast initial membrane association, structural reorganization of α-helical segments of PLA2 takes place at the lipid water interface. Obtained rate constants displayed an about 2-fold increase of the slower component for the all-fluid DOPC/DOPG mixture compared to that of the heterogeneous raft-like lipid bilayer, which offers more fluid-like hydrolysis-competent phospholipid molecules. FRET-based activity measurements reveal that pressure has a drastic inhibitory effect on the lipid hydrolysis rate, rendering it a potentially effective pressure sensing system. The enzymatic activity of bvPLA2 decreases by ∼75% in the pressure range from 1 to 2000 bar. The reduced activity is largely due to an expansion of the enzyme−substrate structure upon transition state formation, with an activation volume, $\Delta V^{\ddagger}$, of about 13−26 mL mol^{-1}, which is in the order of 1−2 water molecules, only. Additionally, a decrease in membrane fluidity upon compression may impede conformational changes accompanying various reaction steps, thereby reducing the rate of the overall reaction bvPLA2.

The study of membrane-bound proteins such as PLA2 using HHP modulation clearly has the potential to provide novel information regarding molecular interactions that cause a protein to bind to membranes and their associates with other proteins on the membrane surface, also for extreme environmental conditions. Hence, these results also deepen our understanding of membrane-associated pressure effects on phospholipase-controlled processes in deep-sea organisms, where pressures up to the kbar-level are encountered. Next to being a primary osmosensor, PLA2 is prone to sense high hydrostatic pressure as well, leading, by its changes in activity, to changes in signaling transduction cascades involved in accumulation and activation of ion channels and of compatible osmolytes and, thus, also to changes in cell volume.

MATERIALS AND METHODS

Materials. The phospholipids 1,2-dioleoyl-*sn*-glycero-3-phosphocholine (DOPC), 1,2-dioleoyl-*sn*-glycero-3-phospho-(1′-*rac*-glycerol) sodium salt (DOPG), 1,2-dipalmitoyl-*sn*-glycero-3-phosphocholine (DPPC), 1,2-dipalmitoyl-*sn*-glycero-3-phospho-(1′-rac-glycerol) sodium salt (DPPG) were purchased from Avanti Polar Lipids (Alabaster, USA). The fluorescent lipids 2-(3-(diphenylhexatrienyl)-propanoyl)-1-hexadecanoyl-*sn*-glycero-3-phosphocholine (β-DPH HPC) and O-(6-DABCYL-aminohexanoyl)-2-*O*-(12-(5-BODIPY-enanoyl)-aminododecanoyl)-*sn*-glyceryl phosphatidylcholine (DBPC)

DOI: 10.1021/jacs.5b07009
J. Am. Chem. Soc. 2015, 137, 12588−12596

were from Setareh Biotech (Eugene, OR, USA) and Echelon Biosciences (Salt Lake City, UT, USA), respectively. Cholesterol (Chol) and Phospholipase A_2 from honey bee venom (Apis mellifera), bvPLA2, was obtained from Sigma-Aldrich (Deisenhofen, Germany).

High-Pressure FTIR Spectroscopy. The pressure-dependent FTIR spectra were recorded using a Nicolet 6700 IR spectrometer equipped with liquid nitrogen cooled MCT (HgCdTe) detector (Thermo Fisher Scientific Inc., MA, USA). The infrared light was focused by a spectral bench onto the pinhole of a diamond anvil cell (with type IIa diamonds from Diamond Optics) as described previously.[61] FTIR measurements have been carried out in D_2O as the solvent to avoid spectral overlap of the amide I′ band with the bending mode of H_2O. For H/D exchange bvPLA2 was kept in pure D_2O for 5 h. After lyophilization, protein (2 wt %) was hydrated with 20 mM bis-Tris buffer, pD = 8.0, 100 mM NaCl, 15 mM KCl, 2 mM $CaCl_2$ or 0.5 mM EGTA in the presence of vesicles (protein to lipid molar ratio 1:40). Large unilamellar vesicles, after five freeze−thaw−vortex cycles, were formed by extrusion through polycarbonate membranes of 100 nm pore size at 65 °C.[25] Spectral analysis was carried out using Grams software (Thermo Electron Corp., MA, USA). Secondary structure estimation was performed by fitting subbands to the amide I′ band, whose peak wavenumbers are characteristic for the secondary structure elements, and areas are proportional to their fractions. Initial peak wavenumbers for the fitting analysis were picked from second derivative spectra and by Fourier self-deconvolution (FSD).

Ambient Pressure Stopped-Flow Measurements. Fast kinetics measurements of bvPLA2 membrane binding and activity at atmospheric pressure were performed using an SX18 MV stopped-flow spectrometer (Applied Photophysics, Leatherhead, UK) by rapid mixing of 0.35 μM bvPLA2 with liposomes of varying concentration. In the binding experiment, fluorescence of the intrinsic tryptophans of bvPLA2 was excited at 280 nm filter using a slit width of ±1 nm. Fluorescence emission of the lipid β-DPH HPC dye resulting from FRET with bvPLA2 was recorded through a 420 nm cutoff filter. Typically, 5−8 single injections were accumulated for each experimental condition, monitored over 2 s binding reaction time. Unless indicated otherwise, all binding measurements were performed at 37 °C in buffer containing 20 mM Tris/HCl, pH 8.0, 0.5 mM EGTA to avoid vesicle hydrolysis during the fluorescent measurements. The observed association rate constants were obtained from fits assuming multiphasic exponential processes; typically, a biphasic time course displayed a sufficient approximation of the experimental data. The lipid concentration was chosen to be much higher (>100×) than the concentration of the protein, to be able to analyze the data in terms of a pseudo-first-order association model in which the phospholipid concentration is rate-determining.

In the catalysis experiment, a fluorogenic analogue of the PLA_2 substrate PC, named DBPC (O-(6-DABCYL-aminohexanoyl)-2-*O*-(12-(5-BODIPY-entanoyl)aminododecanoyl)-*sn*-glyceryl phosphatidylcholine), was used.[62] In this fluorescence dequenching assay, the DBPC molecule, containing the quencher DABCYL, via intramolecular energy transfer, quenches emission of the excited BODIPY fluorescent dye when the phospholipid substrate is not hydrolyzed. Loss of this intramolecular spatial correlation of the two fluorophores in DBPC by hydrolysis of the *sn*-2 acyl chain results in strong enhancement of fluorescence of BODIPY attached to the released lyso-fatty acid analogue. This increase of fluorescence emission of the BODIPY dye resulting from release of the reaction product was recorded for 100 s through a 530 nm cutoff filter, after excitation at 488 nm. All enzyme activity measurements were performed at 37 °C in buffer containing 20 mM Tris/HCl, pH 8.0, 5 mM $MgCl_2$, 2 mM $CaCl_2$.

High Pressure Stopped-Flow Measurements. Rapid reaction pressure-dependent kinetic experiments of binding and activity were both monitored by means of a Hi-Tech Scientific HPSF-56 high-pressure stopped-flow spectrophotometer (TgK Scientific, Bradford on Avon, U.K.) at pressures between 1 and 2000 bar. The syringe assembly of the high-pressure stopped-flow unit is mounted inside a high-pressure vessel that has pressure-stable sapphire windows for the entering and fluorescence light. The dead time of the system is <10 ms (for details of the instrument and setup see the literature[63]). Measurements of the enzymatic activity were carried out under conditions that confer to a pseudo-first-order reaction kinetic behavior by using 0.35 μM bvPLA2 and 98.2 μM lipid vesicles. Typically, 3−6 reaction traces were measured at each pressure condition with an interval of 400 bar. We confirmed that the application of pressure had an insignificant effect on the emission of released BODIPY upon hydrolysis, increasing the initial baseline signal of the lipid vesicles, only, which was corrected for in the final data analysis.

■ ASSOCIATED CONTENT

Supporting Information

The Supporting Information is available free of charge on the ACS Publications website at DOI: 10.1021/jacs.5b07009.

Experimental data and a detailed description of the AFM data analysis. (PDF)

■ AUTHOR INFORMATION

Corresponding Author

*roland.winter@tu-dortmund.de

Notes

The authors declare no competing financial interest.

■ ACKNOWLEDGMENTS

Financial support from the DFG Research Unit FOR 1979, the International Max Planck Research School in Chemical Biology (IMPRS-CB) and in part by the Cluster of Excellence RESOLV (EXC 1069) is gratefully acknowledged. We would also like to thank Dr. Matthias P. Müller (MPI Dortmund) for stimulating discussions.

■ REFERENCES

(1) Staubach, S.; Hanisch, F.-G. *Expert Rev. Proteomics* **2011**, *8*, 263−277.

(2) Bethani, I.; Skanland, S. S.; Dikic, I.; Acker-Palmer, A. *EMBO J.* **2010**, *29*, 2677−2688.

(3) van den Brink-van der Laan, E.; Killian, J. A.; Kruijff, B. de. *Biochim. Biophys. Acta* **2004**, *1666*, 275−288.

(4) Lambeau, G.; Gelb, M. H. *Annu. Rev. Biochem.* **2008**, *77*, 495−520.

(5) Scott, D. L.; Otwinowski, Z.; Gelb, M. H.; Sigler, P. B. *Science* **1990**, *250*, 1563−1566.

(6) Tatulian, S. A. *Biophys. J.* **2001**, *80*, 789−800.

(7) Burack, W. R.; Biltonen, R. L. *Chem. Phys. Lipids* **1994**, *73*, 209−222.

(8) Berg, O. G.; Gelb, M. H.; Tsai, M. D.; Jain, M. K. *Chem. Rev.* **2001**, *101*, 2613−2654.

(9) Dennis, E. A.; Cao, J.; Hsu, Y.-H.; Magrioti, V.; Kokotos, G. *Chem. Rev.* **2011**, *111*, 6130−6185.

(10) Jackman, J. A.; Cho, N.-J.; Duran, R. S.; Frank, C. W. *Langmuir* **2010**, *26*, 4103−4112.

(11) Krajewska, B.; van Eldik, R.; Brindell, M. *JBIC, J. Biol. Inorg. Chem.* **2012**, *17*, 1123−1134.

(12) Brooks, N. J. *IUCrJ* **2014**, *1*, 470−477.

(13) Kapoor, S.; Triola, G.; Vetter, I. R.; Erlkamp, M.; Waldmann, H.; Winter, R. *Proc. Natl. Acad. Sci. U. S. A.* **2012**, *109*, 460−465.

(14) Silva, J. L.; Foguel, D.; Royer, C. A. *Trends Biochem. Sci.* **2001**, *26*, 612−618.

(15) Lendermann, J.; Winter, R. *Phys. Chem. Chem. Phys.* **2003**, *5*, 1440−1450.

(16) Kraineva, J.; Narayanan, R. A.; Kondrashkina, E.; Thiyagarajan, P.; Winter, R. *Langmuir* **2005**, *21*, 3559−3571.

(17) Mishra, R.; Winter, R. *Angew. Chem., Int. Ed.* **2008**, *47*, 6518−6521.

(18) Hochachka, P. W.; Somero, G. N. *Biochemical Adaptation. Mechanism and Process in Physiological Evolution*; Oxford University Press: New York, 2002.
(19) Tzima, E. *Circ. Res.* **2006**, *98*, 176−185.
(20) Siebenaller, J. F.; Garrett, D. J. *Comp. Biochem. Physiol., Part B: Biochem. Mol. Biol.* **2002**, *131*, 675−694.
(21) Myers, K. A.; Rattner, J. B.; Shrive, N. G.; Hart, D. A. *Biochem. Cell Biol.* **2007**, *85*, 543−551.
(22) Abe, F.; Kato, C.; Horikoshi, K. *Trends Microbiol.* **1999**, *7*, 447−453.
(23) Winter, R.; Jeworrek, C. *Soft Matter* **2009**, *5*, 3157−3173.
(24) Scarlata, S. *Braz. J. Med. Biol. Res.* **2005**, *38*, 1203−1208.
(25) Kapoor, S.; Werkmuller, A.; Denter, C.; Zhai, Y.; Markgraf, J.; Weise, K.; Opitz, N.; Winter, R. *Biochim. Biophys. Acta, Biomembr.* **2011**, *1808*, 1187−1195.
(26) Dennis, E. A. *J. Biol. Chem.* **1994**, *269*, 13057−13060.
(27) Six, D. A.; Dennis, E. A. *Biochim. Biophys. Acta, Mol. Cell Biol. Lipids* **2000**, *1488*, 1−19.
(28) Dennis, E. A.; Rhee, S. G.; Billah, M. M.; Hannun, Y. A. *FASEB J.* **1991**, *5*, 2068−2077.
(29) Zhang, Y.; Lemasters, J.; Herman, B. *J. Biol. Chem.* **1999**, *274*, 27726−27733.
(30) Qu, X. D.; Lehrer, R. I. *Infect. Immun.* **1998**, *66*, 2791−2797.
(31) Fonteh, A. N.; Bass, D. A.; Marshall, L. A.; Seeds, M.; Samet, J. M.; Chilton, F. H. *J. Immunol.* **1994**, *152*, 5438−5446.
(32) Dzwolak, W.; Kato, M.; Taniguchi, Y. *Biochim. Biophys. Acta, Protein Struct. Mol. Enzymol.* **2002**, *1595*, 131−144.
(33) Pande, A. H.; Qin, S.; Nemec, K. N.; He, X.; Tatulian, S. A. *Biochemistry* **2006**, *45*, 12436−12447.
(34) Tatulian, S. A.; Biltonen, R. L.; Tamm, L. K. *J. Mol. Biol.* **1997**, *268*, 809−815.
(35) Shan, S. O.; Loh, S.; Herschlag, D. *Science* **1996**, *272*, 97−101.
(36) Gerlach, H.; Laumann, V.; Martens, S.; Becker; Christian, F. W.; Goody, R. S.; Geyer, M. *Nat. Chem. Biol.* **2010**, *6*, 46−53.
(37) Ghomashchi, F.; Lin, Y.; Hixon, M. S.; Yu, B. Z.; Annand, R.; Jain, M. K.; Gelb, M. H. *Biochemistry* **1998**, *37*, 6697−6710.
(38) Bollinger, J. G.; Diraviyam, K.; Ghomashchi, F.; Murray, D.; Gelb, M. H. *Biochemistry* **2004**, *43*, 13293−13304.
(39) Eisenblätter, J.; Winter, R. *Biophys. J.* **2006**, *90*, 956−966.
(40) Berg, O. G.; Yu, B. Z.; Rogers, J.; Jain, M. K. *Biochemistry* **1991**, *30*, 7283−7297.
(41) Yu, B. Z.; Ghomashchi, F.; Cajal, Y.; Annand, R. R.; Berg, O. G.; Gelb, M. H.; Jain, M. K. *Biochemistry* **1997**, *36*, 3870−3881.
(42) Tong, Y.; Li, N.; Liu, H.; Ge, A.; Osawa, M.; Ye, S. *Angew. Chem., Int. Ed.* **2010**, *49*, 2319−2323.
(43) Snitko, Y.; Koduri, R. S.; Han, S. K.; Othman, R.; Baker, S. F.; Molini, B. J.; Wilton, D. C.; Gelb, M. H.; Cho, W. *Biochemistry* **1997**, *36*, 14325−14333.
(44) Mouritsen, O. G.; Andresen, T. L.; Halperin, A.; Hansen, P. L.; Jakobsen, A. F.; Jensen, U. B.; Jensen, M. O.; Jørgensen, K.; Kaasgaard, T.; Leidy, C.; Simonsen, A. C.; Peters, G. H.; Weiss, M. *J. Phys.: Condens. Matter* **2006**, *18*, S1293−304.
(45) Simonsen, A. C. *Biophys. J.* **2008**, *94*, 3966−3975.
(46) Schuabb, V.; Czeslik, C. *Langmuir* **2014**, *30*, 15496−15503.
(47) Singer, A. G.; Ghomashchi, F.; Le Calvez, C.; Bollinger, J.; Bezzine, S.; Rouault, M.; Sadilek, M.; Nguyen, E.; Lazdunski, M.; Lambeau, G.; Gelb, M. H. *J. Biol. Chem.* **2002**, *277*, 48535−48549.
(48) Leidy, C.; Mouritsen, O. G.; Jorgensen, K.; Peters, G. H. *Biophys. J.* **2004**, *87*, 408−418.
(49) Brooks, N. J.; Ces, O.; Templer, R. H.; Seddon, J. M. *Chem. Phys. Lipids* **2011**, *164*, 89−98.
(50) Kinkaid, A.; Wilton, D. C. *Biochem. J.* **1991**, *278*, 843−848.
(51) Tatulian, S. A.; Qin, S.; Pande, A. H.; He, X. *J. Mol. Biol.* **2005**, *351*, 939−947.
(52) Wagner, K.; Brezesinski, G. *Curr. Opin. Colloid Interface Sci.* **2008**, *13*, 47−53.
(53) Teng, Q.; Scarlata, S. *J. Biol. Chem.* **1993**, *268*, 12434−12442.
(54) Rebecchi, M.; Bon Homme, M.; Scarlata, S. *Biochem. J.* **1999**, *341*, 571−576.
(55) Lehtonen, J. Y.; Kinnunen, P. K. *Biophys. J.* **1995**, *68*, 1888−1894.
(56) Winter, R.; Dzwolak, W. *Philos. Trans. R. Soc., A* **2005**, *363*, 537−563.
(57) Ulrich, A. S.; Sami, M.; Watts, A. *Biochim. Biophys. Acta, Biomembr.* **1994**, *1191*, 225−230.
(58) Masson, P.; Balny, C. *Biochim. Biophys. Acta, Gen. Subj.* **2005**, *1724*, 440−450.
(59) Scott, D. L.; White, S. P.; Otwinowski, Z.; Yuan, W.; Gelb, M. H.; Sigler, P. B. *Science* **1990**, *250*, 1541−1546.
(60) Tatulian, S. A. *Biophys. J.* **2003**, *84*, 1773−1783.
(61) Panick, G.; Malessa, R.; Winter, R.; Rapp, G.; Frye, K. J.; Royer, C. A. *J. Mol. Biol.* **1998**, *275*, 389−402.
(62) Feng, L.; Manabe, K.; Shope, J. C.; Widmer, S.; DeWald, D. B.; Prestwich, G. D. *Chem. Biol.* **2002**, *9*, 795−803.
(63) Bugnon, P.; Laurenczy, G.; Ducommun, Y.; Sauvageat, P. Y.; Merbach, A. E.; Ith, R.; Tschanz, R.; Doludda, M.; Bergbauer, R.; Grell, E. *Anal. Chem.* **1996**, *68*, 3045−3049.

DOI: 10.1021/jacs.5b07009
J. Am. Chem. Soc. 2015, 137, 12588−12596